Available online at www.sciencedirect.com

ScienceDirect

Procedia Engineering 2 (2010) 2131–2140

Procedia Engineering

www.elsevier.com/locate/procedia

Fatigue 2010

X-ray computed μ-tomography: a tool for the characterization of fatigue defect population in a polychloroprene rubber

Y. Marco[a,]*, V. Le Saux[a], S. Calloch[a], P. Charrier[b]

[a]*LBMS EA4325 ENSIETA/UBO/ENIB/Université Européenne de Bretagne, 2 rue F. Verny, 29806 Brest Cedex 9, France*
[b]*Trelleborg Modyn, Z.I. Nantes Carquefou BP419, 44474 Carquefou Cedex, France*

Received 24 February 2010; revised 9 March 2010; accepted 15 March 2010

Abstract

As elastomeric materials are heterogeneous by nature, their fatigue behavior is strongly driven by the initiation and the growth of cavities. The explanations on the microscopic mechanisms are usually supported by SEM observations. SEM is a 2D destructive technique that can induce artifacts and is not suitable to analyze 3D phenomena. Moreover, the time needed to observe a single slice prevents from scanning a whole massive sample. In this study X-ray micro-tomography is used. This non destructive method has already been widely applied to elastomeric materials to control the fillers size and dispersion or to analyze the cavitation induced under high hydrostatic pressure fatigue loading, for example. Here, this technique is used with a good resolution to analyze the evolution of the defects population during a fatigue campaign on hourglass-shaped specimens. The initiation and propagation mechanisms are clearly illustrated on 3D observations, and the influences of the maximum principal strain and of the number of cycles on several damage parameters (size repartition, porosity, defect volumic density) are investigated. A scenario for the fatigue damage evolution is proposed and some fatigue initiation criteria are finally discussed with the help of the micro-structural measurements.

Keywords: fatigue analysis; microstructure; X-ray micro-tomography; elastomer

1. Introduction

The use of elastomeric parts is today very widespread in all industrial markets, to fulfil very different requirements (static or dynamic tightness, damping of vibrations or shocks, high chemical resistance…). If the design of static or dynamic requirements is today well mastered, the field experience underlines that the two main failure mechanisms are related to fatigue and ageing. For a dozen years, coupled studies of industrials and academic partners allowed to propose several criteria to evaluate the fatigue lifetime of an elastomeric structure. But the requirements for higher durability for even more severe conditions lead now to overcome the next difficulty, which is the understanding of the links between the process and the fatigue properties. These links are still not well understood for several reasons: the deformations encountered are extremely large, the material is obtained from a recipe mixing several components, its properties depend on the curing and injection parameters and the phenomena

* Corresponding author. Tel.: +33 (0)2 98 34 89 11; fax: +33 (0)2 98 34 87 30.
E-mail address: Yann.Marco@ensieta.fr.

1877-7058
doi:10.1016/j.proeng.2010.03.229

involved couple mechanical, thermal and chemical effects, etc. [1,2]. In this paper, the influence of the mechanical parameters on the fatigue resistance is investigated, with as less as possible coupled effects like ageing or crystallization. Coming from the heterogeneous nature of elastomeric materials (fillers, oxides, additives, natural inclusions, etc.) the fatigue properties are strongly dependant on the existing flaws, which can be considered as the main sites for damage initiation [3]. The roles of these flaws are usually studied by SEM analysis [4,5], which provide interesting data but can hardly be representative of the global damage [6]. In this study, we will use X-ray micro-tomography (X-ray CT). This non-destructive observation technique enables to study 3D imaging of material microstructures [7] as well as pore distributions [8]. The technique has also proven to be a useful tool in assessing the micro-mechanisms of fatigue crack growth [9] and damage evolution [10]. Dealing with elastomeric materials, a few studies already exists either dedicated to the observation of inclusions dispersion or to the damage evolution. On the last point, remarkable works were done during the last years, proving how useful this technique could be to study the cavitation at a mesoscopic scale for high hydrostatic fatigue conditions [2] or to detect local change of physical and chemical properties by measuring X-ray attenuation [11]. Unfortunately, the quite low resolution (about 200µm) of the medical scanner usually used prevents the detection of small defects (about 40µm) that are associated to the fatigue initiation [12]. One of the most interesting article on the use of X-ray CT to follow the damage evolution has been published recently [8] and provides very useful informations on the fatigue mechanisms with a higher resolution (detection of defects with a diameter of about 15µm). Nevertheless, quantitative data describing the dependency of the defect population on the fatigue parameters are still missing, which prevents from proposing or validating the existing models trying to describe the initiation and the growth of fatigue cavities. It is especially clear that if the basic mechanisms for fatigue have been identified (polar decohesion, cavitation, inclusions break), the understanding of the early stages of fatigue and of the damage scenarios leading to a macroscopic crack are still wide opened issues. The purpose of this paper is therefore to use computed X-ray micro-tomography with a high enough resolution (detection of defects with a radius of about 13µm) to describe in a 3D manner the fatigue mechanisms and to propose a description of the evolution of the defect population in a polychloroprene rubber submitted to fatigue loading. This technique is used here to analyze hourglass shaped samples previously submitted to several fatigue loading conditions. The initiation and propagation mechanisms are investigated. Then, the influences of the maximum local strain and of the number of cycles on representative parameters (cavities distribution, average volume, porosity, volumic number of defects) are studied and a scenario is proposed for the damage evolution. Based on these results, an evaluation of some basic fatigue criteria is proposed.

2. Materials and testing

2.1. Materials and specimen

The material used here is a polychloroprene rubber (CR) formulated with silica and a low percentage of carbon black. Hourglass shaped specimens were manufactured from a single batch in order to ensure the reliability of mixing and moulding conditions. The geometry of the specimen is given on Figure 1. This kind of specimen (called AE2 in the following) was chosen for three main reasons: it is classically used to obtain Wöhler curves; the initiation and break zone is well mastered and is located in the thinner section; its complex geometry leads to different strain and stress states along its axis, even under uni-axial tensile tests, and will make the X-ray CT analysis richer.

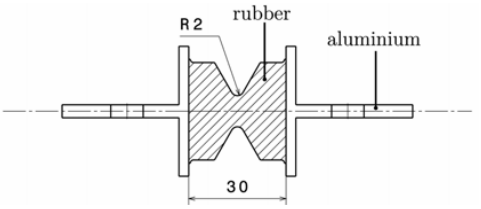

Fig. 1. AE2 specimen

2.2. Micro-tomography and analysis

The goal of this study is to analyze a large enough volume in order to be representative of the fatigue damage scenarios. The device must be powerful and characterized by a resolution high enough compared to the defect sizes classically measured by SEM measurements (ranging from 10 to 400µm). The experimental settings of the Phoenix device used (v|tome|x L 240) are given in table 2.

Tab. 1. X-ray tomography experimental settings

X-ray tube voltage	180kV
current	116µA
scan time	≈30min
rotation	360° by step of 0.45°
resolution	1px = 21µm

More details on the experimental settings can be found in [13]. All the specimens were slightly stretched (relative displacement of 2mm of the inserts) in order to open the cavities and to make them easier to detect. This stretching was carefully achieved just before the measurement in order to prevent the opening of the cavities under static conditions during the time left between the mechanical test and the X-ray CT observation. Coming from the image analysis parameters chosen to avoid artifacts, the smallest defect detected has an equivalent radius of 13 µm.

It is important to notice that, in this study, no samples were submitted again to fatigue loading after the X-ray CT measurements. This choice implies that no specific defects can be followed as the number of cycles increases, but makes sure that the exposition to X-ray is not influencing the material behaviour. Moreover, comparing several specimens gave us the possibility to take the intrinsic dispersion in the fatigue properties into account.

2.3. Fatigue campaign

Fatigue tests were conducted at room temperature, on an INSTRON 1342 hydraulic machine, equipped with hydraulic grips. The frequency of the tests was set to 2 Hz in order to limit the heat build-up effect and the experiments were displacement controlled. The load ratio was fixed to R=0 in order to limit the low crystallization effect that may be encountered for polychloroprene rubber [2].

First, several fatigue tests were conducted to build a Wöhler curve with AE2 specimens, with the formerly detailed settings. Five specimens were tested at five strain levels. During the tests, the stiffness and the specimen temperature were recorded and a classical criterion on the stiffness loss rate [14] was used to detect the initiation (associate to a micro-crack of about 2 mm). The Wöhler curve obtained is presented on figure 2.

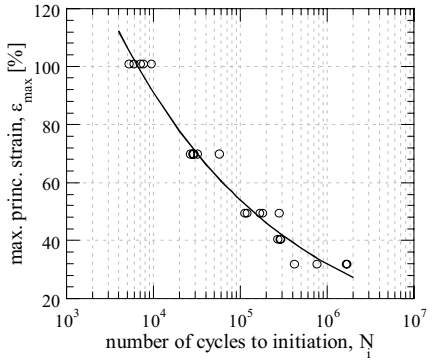

Fig. 2. Wöhler curve of the studied material (R=0@2Hz)

Then, 3 macroscopic maximum displacements (2, 4 and 6mm) were chosen, associated with the respective numbers of cycles that lead to initiation, noted Ni in the following. For each of these displacements, at least 5 interrupted tests were achieved (some of them were made twice) stopped after 5 cycles and after 10, 25, 50, 100% of Ni (identified on the Wöhler curve). Those samples were then analyzed using X-ray CT.

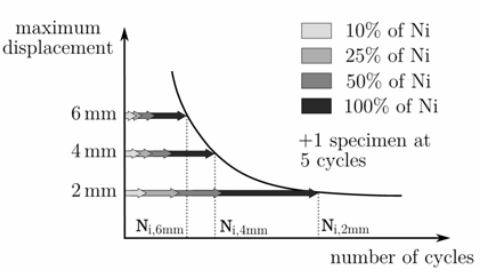

Fig. 3. Interrupted fatigue tests

3. Results

Figure 4 shows a typical result obtained by X-ray CT on a sample with no clear cracks but exhibiting a large number of cavities. Even if this figure is very interesting, its representation is too global to give accurate hints on the initiation and propagation mechanisms. In this paragraph, we will zoom on specific representative defects in order to illustrate the geometry of the fatigue initiation sites, and on a few cracks, illustrating the propagation scenarios from their 3D geometry. In Paragraph 3.2, a more systematic analysis will be performed on the features of the defect population observed.

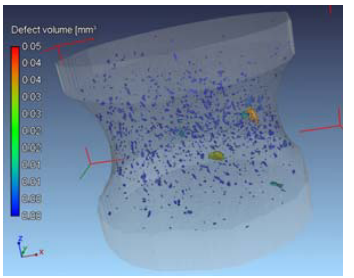

Fig. 4. Example of cavities mapping obtained with X-ray µ-tomography

3.1. Illustration of the initiation and propagation mechanisms

Cavities were found to initiate from existing flaws in the material, either inclusions or agglomerates, which is a classic result for fatigue. The most often encountered inclusions and agglomerates in the studied material are ZnO (white spots, density=5.6g/cm^3), SiO2 (gray agglomerates, density=2.2g/cm^3) and carbon blacks (dark spots, density=1.9g/cm^3). The observations lead to identify the main damage processes that can be classified into three categories:

- Voids are created between two or more close flaws oriented along the tensile direction, whatever the nature of the involved particles (ZnO, SiO2 and carbon black), as illustrated on Figure 5a. This mechanism is the most often encountered and can be related to the high hydrostatic local conditions encountered in these zones. In a few cases, cavitation is also observed after preliminary break of agglomerates;

- Voids are created in the polar zones of inclusions (Fig. 5b). This case was mainly found in isolated inclusions;
- Some voids are observed without any clear agglomerates inclusions in their neighborhood. This could either be explained by flaws with a radius smaller than 13µm, thus not detected due to the resolution of our device, or from carbon black agglomerates that are always difficult to point out clearly because they have nearly the same density as the matrix.

Using global overviews for the samples observed, we can point out that there is no defect apparition preferential zones (for example a ring near the surface sample or specific location due to the injection pin point) and that no clear influence of the process can be involved (except for the presence of agglomerates that can hardly be avoided by any type of mixing process). This last point will be further investigated as the injection point location, the flow history and the mould parting zone are very likely to influence the inclusions spatial repartition, which may be related to voids smaller than the ones detected in this study.

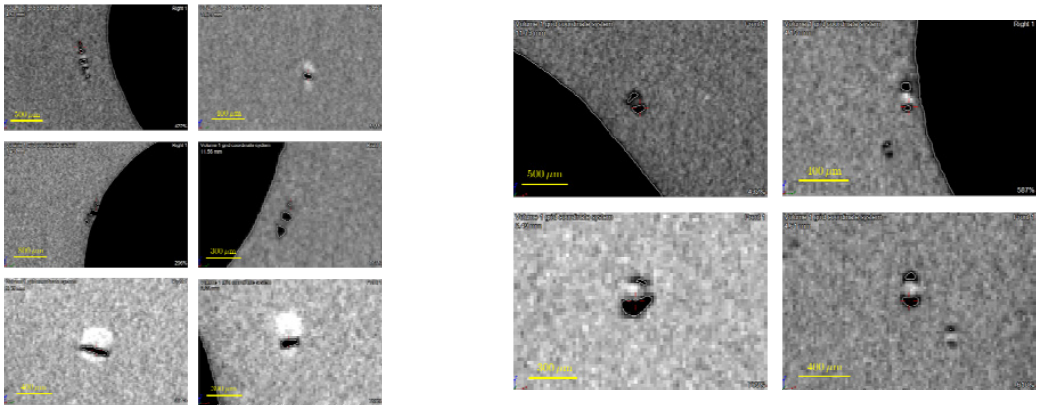

(a) (b)

Fig. 5. Some examples of initiation mechanisms

The present observations meet the conclusions obtained from SEM measurements [3]. Depending on the strength of the link between the inclusion and the matrix, the voids will be created at the interface (decohesion) or in the matrix (cavitation). It also shows that the probability to observe cavitation between close particles, well aligned with the solicitation axis, is higher than around large size inclusions, confirming a recent study achieved on carbon black filled NR [6] using the same technique. This means that fatigue damage modeling using finite elements analysis has to consider several inclusions to be representative (not talking about shape or gradient effects). It is interesting to note that the sizes of these big defects, early created, are well correlated to the size of the initiation defects evaluated using inverse approaches based on fracture mechanics [12].

X-ray CT results can also be used to analyze the propagation mechanisms because X-ray result is a “picture” at a given time of the microstructure state. The pictures presented here are showing several radial spatial slices of the same cracks (and not the evolution of some cracks along time). Figure 6 summarize the main observations that can be done. The cracks start usually from a big defect or from the coalescence of several small cavities, always located near the specimen surface (Fig. 6a). Once started, the crack propagates usually at right angle to the direction of solicitation, *i.e.* in mode I. The crack then meets formerly created cavities that are disturbing locally the crack tip orientation but with a main propagation direction remaining the same. A notable exception is illustrated on Figure6b and shows that the existing cavities may guide the propagation along a different direction for fatigue tests at low amplitude. It is interesting to note that the rough surface usually observed by SEM observations is clearly explained here by the progressive opening of pre-existing cavities, which is a mechanism that has already been proposed by Gent and Pulford [15]. Moreover, some ligaments remaining on the border of the cracks are also observed, coming from the cavities geometry and that may be explained by locally induced crystallization [5]. One important point is that we have not observed any specific porosity at the crack tip. It seems (which is conclusion limited by the

smallest defect size detectable) that the crack is just helping the existing cavities to open until they break and that the crack does not create any new defects, as it was proposed by Tsunoda *et al.* [16] or Le Cam *et al.* [5].

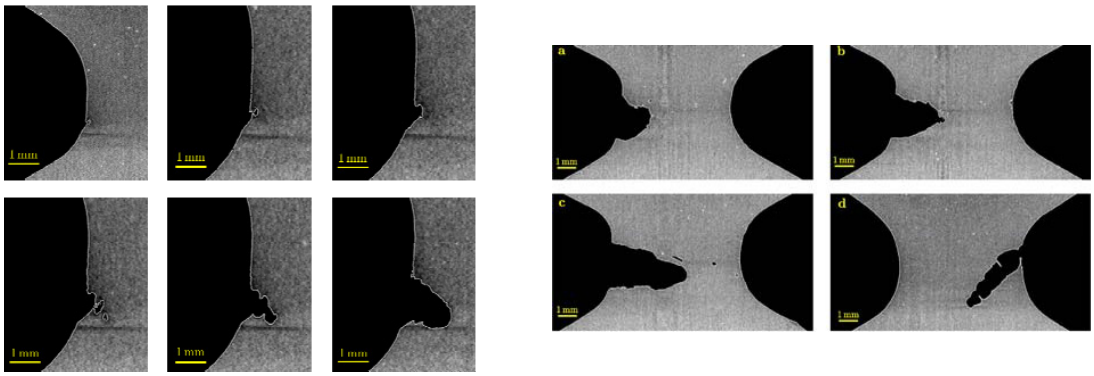

(a) (b)

Fig. 6. Examples of crack propagation

3.2. Dependency of the features of the cavities population on the maximum local strain and on the number of cycles

In the previous section, we shortly described the initiation and propagation mechanisms. We now go further in the analysis with a statistical analysis of the fatigue defect population. Before presenting this analysis, we first define the parameters chosen and to describe of the fatigue damage.

3.2.1. Defect population description

For the description of the defect populations, various parameters can be followed. We focused in this study on 4 parameters, supposed to be relevant to characterize the fatigue damage and classically used as damage variable for modelling:

1. The average radius of a sphere which volume is calculated as the average volume of the defects population;
2. The defect volumic density, *i.e.* the number of defects in a slice, divided by the volume of the slice;
3. The porosity, calculated as the ratio between the sum of the cavity volume in a slice and the volume of the slice;
4. The maximum size of a defect (given in mm^3) encountered in the slice.

What should also be pointed out is that all the samples were obtained from the same batch. They therefore should exhibit the same initial average population of inclusions and agglomerates. Moreover, as the samples were stretched at the same displacement during the X-ray CT, this is not disturbing the evaluation of the defect sizes. In some cases, the samples presented some clear cracks. The formerly presented features were then evaluated from (and rated to) the remaining not cracked volume. The crack tip zone is therefore ignored but this still gives a good evaluation of the defects encountered in the sample. The choice of the local maximum strain is there again enforced as it depends much less on the remaining tested section than stress does and because the tests were displacement controlled.

3.2.2. Population features dependency on elongation and number of cycles

The analysis will be based on the figures 7 and 8 and is just an overview of a complete study [13]. As the specimens are heterogeneous, we have chosen to analyze the results for different volumes of interest characterized by a height of 1mm (referred to as slices 1 to 4). Figure 7 presents the evolution of the chosen parameters with respect to the maximum principal strain of the considered slice. These data are obtained for various numbers of

cycles (except results obtained after 5 cycles) and for the four slices. If we first consider the defect volumic density (fig. 7c), one can observe that its value is strongly dependent on the maximum local strain. It is very interesting to note that the results obtained for the slices of all the tested samples are plotted together, showing a very good agreement for a same local maximum strain. We can also observe that this parameter is dependant on the number of cycles as shown on figure 8. An important increase is observed at the beginning of the experiment and this increase seems to reach a stabilized value before the initiation (the defect volumic density is almost stable after 10% of the initiation time).

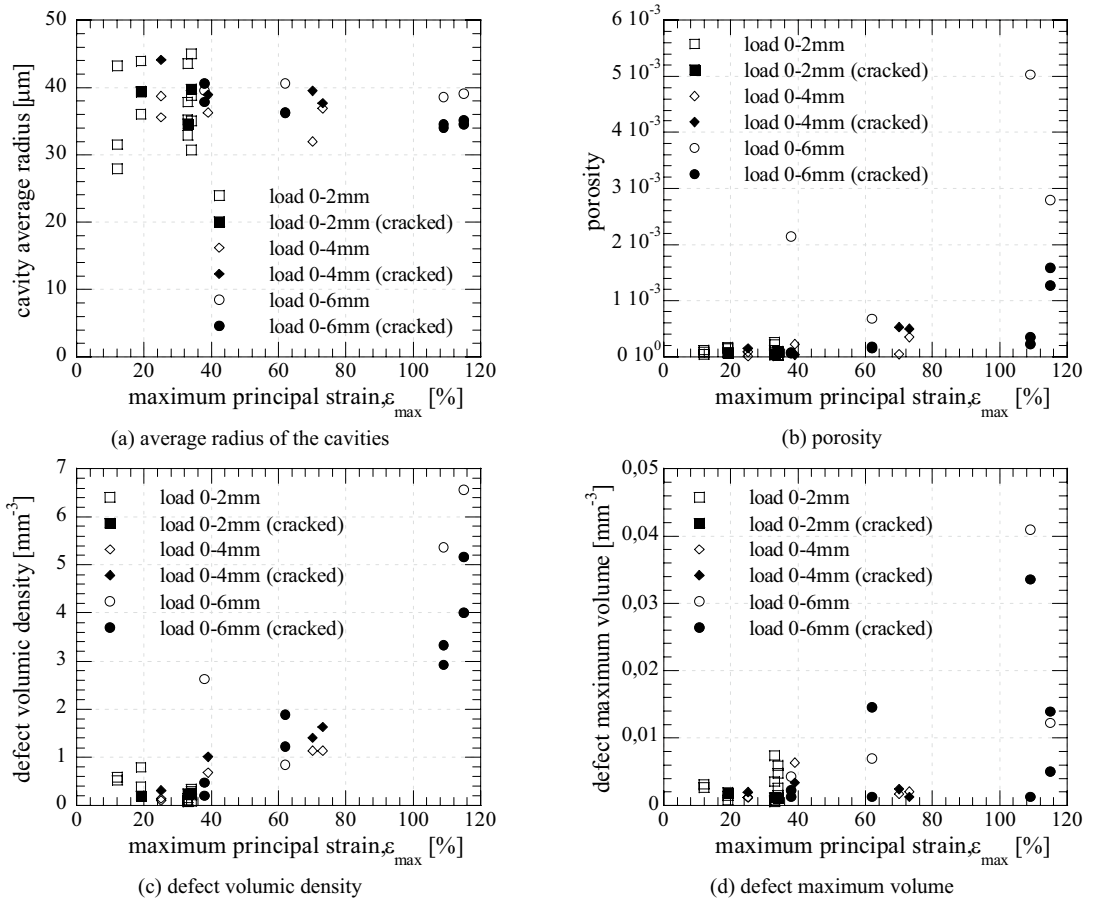

Fig. 7. Evolution of the chosen parameters as a function of the maximum local strain of the considered slice.

Dealing with the average defect radius, it can be observed that it is not much dependent on the local strain. It also seems that increasing the elongation reduces the dispersion observed between the different samples. This observation is only a consequence of the averaged nature of that parameter: as the defects are less numerous for low elongations, large sized cavities have a higher influence. The fact that the average radius remains nearly constant means that the size distribution keeps the same shape. This also means that one can not conclude, from a first sight analysis, that the equivalent radius of the cavities is not evolving along the fatigue cycles because in a sample presenting numerous defects, the growth, even important, of a few of them will not influence much the average radius. As the same cavities are not followed along time, the answers about the growth of the cavities are not as clear as for defects initiation. Figure 7d shows that the maximum volume encountered changes a lot. It appears that

this growth occurs mainly during the first 10% of the initiation lifetime and the growth rates of these big defects are clearly very dependant on the global displacement or maximum local elongation. The evolution of the porosity is related both to the number and to the size of the defects and the logical induced evolutions are observed on Fig. 7b. It seems that the porosity is less sensible to the maximum size than to the number of defects.

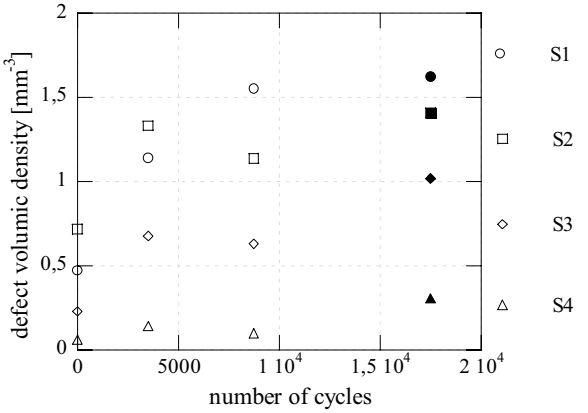

Fig. 8. Evolution of the defect volumic density with respect to the number of cycles of the different slices after cycles at a maximum displacement of 4mm.

4. Discussion

4.1. Discussion on the evolution of the populations

The results presented in section 3 first confirm the initiation mechanisms observed from SEM observations. Some specific comments can be pointed out such as the high proportion of cavities initiated between close inclusions, whatever their nature, and the fact that the defect volumic density does not seem to be higher at the crack tip, even if the existing cavities are opened wider. Some defects are created very early during the fatigue tests: 5 cycles are enough to initiate them, but they do not propagate yet. A clear dependency of the number of defects initiated on the global displacement (and on the local maximum strain) is observed. During the following step of the fatigue tests (until 10% of the initiation lifetime), three main observations can be done: the maximum size encountered drastically increased showing an important growth of some big cavities, the number of defects also increases very much and the average radius remains the same. This first step can therefore be considered as a fast growing period for a few defects, but also as an initiation period for the cavity populations, with only a slow growth, if any, of the large majority of the defects. These results are correlating the observations from SEM observations [5] and for X-ray CT measurements on interrupted fatigue tested specimen [6].

It therefore seems that the number of activated defects in a volume strongly depends on the experienced local strain and reaches a nearly stabilized value in a number of cycles lower than 10% of the initiation lifetime. The growth rates of the big defects as well as the rate of initiation are strongly dependant on the maximum local strain and the dependency of the defects volumic density on this local value is clearly established for different slices taken from different samples. After that first step, the average radius grows slowly, with stabilized values of the defect volumic density and of the maximum volume. It can be concluded that between 10% and 50% of the initiation time (as some samples already present some cracks, it could even be 100% of the initiation duration), the defects are slowly growing, until a local macro-crack appears. There again, clear conclusions on the growth history of the cavities will be only accessible by following a single sample submitted to several interrupted tests, which is to be done in our next investigations by going on with the interrupted samples tested in this study. Still, a global coalescence is not probable to happen during 50% of the initiation time as no drop of the defect volumic density is

observed and because the increase of the average radius remains small: coalescence would in the same time reduces the number of defects and increases their size, and the rise of the average radius along the fatigue cycles would have been much clearer. These observations consequently confirm that coalescence of the defects is occurring very lately [6].

4.2. Discussion on some simple initiation criterion

The number of cycles leading to "initiation" is usually the one used to design massive samples (for thin samples like H2 specimens, the break follows the initiation almost immediately). From a macroscopic point of view, this number of fatigue cycles could be classically identified either as the one leading to an observable crack of 1 to 2mm on the skin of the sample [3], either as the one that leads to a sudden drop of the sample stiffness [14]. From X-ray CT measurements, it is clear that these criteria are limited because enormous inside cavities can be seen, very likely created before the external crack and not associated with a major drop of stiffness, as they did not appear in the thinner zone.

Because the porosity and the defect volumic density measured for the different testing conditions are very different but are leading to the appearance of a macroscopic crack, the initiation criteria of a critical void ratio is excluded. As the defect maximum size changes a lot from one sample to another for a given local maximum strain, we should be tempted to avoid a criteria based on a maximum cavity size. It seems to us that the most convincing criterion should be based on a dissipated energy summed along the fatigue cycles. This dissipated energy is clearly dependant on the matrix dissipation but also on the defect population. In another paper [17,18], we propose a method to evaluate this dissipation from temperature measurement and the population of defects. This approach seems to give reliable results, opening a new field of investigation.

5. Conclusions

The results presented in section 3 and discussed in section 4 first confirm the initiation mechanisms proposed from SEM observations. Two specific points can be underlined: the observation that there is no specifically high density of defects at the crack tip and the high proportion of cavities initiated between close inclusions, whatever their nature. A scenario for the evolution of the defect population can be proposed. The initiations of the cavities happen very early. After only 5 cycles, the final defect density is almost reached for the fatigue tests achieved under a low displacement. Within a number of cycles lower than 10% of the initiation lifetime, an increase in the amount of defects is observed, with no clear increase of their volumes, except for a few of them, under high elongations. This rise of the number of cavities is strongly related to the global displacement and to the maximum local strain. Afterward, the number of defects increases very slowly along the fatigue test and is coupled with an overall slow growth of the cavities. No sudden coalescence of the cavities seems to happen, except locally, helping the growth of a low number of defects that becomes micro-cracks, which do not affect the average radius of the global population. The rate growth of these cracks is very dependant on the global displacement, which can be related to the much higher density of defects already created. During this propagation phase, a shielding process of already created voids may happen. The comparison of the results obtained for several global displacements shows that no global criteria can be related to a critical void ratio, as both porosity and number of defects are very different for specimens exhibiting macro-cracks. An energy based criterion seems to be the best choice, even if a critical size based criteria can not be excluded. The perspectives of this work are very numerous, ranging from validation of Finite Element simulations at a microscopic scale to experimental investigations for several load ratio variations, several kind of elastomers, etc.

Acknowledgements

The authors would like to thank the Brittany region for its financial support and all the partners involved in the FEMEM project. A special thank to G. Bourbouze (CRT Morlaix) for performing the tomography measurements.

References

[1] I. Choi and C.M. Roland, *Rubber Chemistry and Technology* 1996; **69**: 591-599.

[2] K. Legorgu-jago and C. Bathias, *Int. J.of Fatigue* 2002; **24**:85-92.

[3] N. Saintier, G. Cailletaud and R. Piques, *Int. J. of Fatigue* 2006; **28**:61-72.

[4] J.J.C. Busfield, A.G. Thomas and M.F. Ngah*, Constitutive Model for Rubber*, Rotterdam (The Netherlands) 1999; **I**:249-256.

[5] J.-B. Le Cam, B. Huneau, E. Verron and L. Gornet, *Macromolecules* 2004, **37**:5011-5017.

[6] K. Le Gorgu Jago*, Constitutive Model for Rubber*, Paris (France) 2007; **V**:173-177.

[7] L. Salvo, P. Cloetens, E. Maire, S. Zabler, J.J. Blandin, J.Y. Buffière, W. Ludwig, E. Boller, D. Bellet and C. Josserond, *Nuclear Instrumentation and Methods in Physics Research B* 2003; **200**:273-286.

[8] J.Y. Buffière, S. Savelli, P.H. Jouneau, E. Maire and R. Fougieres, *Materials Science and Engineering A* 2001; **316**:115-126.

[9] E. Ferrié, J.Y. Buffière, W. Ludwig, A. Gravouil and L. Edwards, *Acta Materialia* 2006, **54**:1111-1122.

[10] M.F. Horstemeyer, K. Gall, K.W. Dolan, A. Waters, J.J. Haskins, D.E. Perkins, A.M. Gokhale and M.D. Dighe, *Theoretical and Applied Fracture Mechanics* 2003; **39**:23-45.

[11] E. Bayraktar, S. Antolonovich and C. Bathias, *International Journal of Fatigue* 2006; **28**:1322-1333.

[12] A.N. Gent, P.B. Lindley and A.G. Thomas, *Journal of Applied Polymer Science* 1964; **8**:455-466.

[13] V. Le Saux, Y. Marco, S. Calloch and P. Charrier, Evaluation of the fatigue defect population in an elastomer using X-ray computed micro-tomography, *J. P. E. S.*, to appear 2010.

[14] E. Ostoja Kuczynski, P. Charrier, E. Verron, L. Gornet and G. Marckmann, *Constitutive Model for Rubber*, London (UK) 2003; **III**:41-48.

[15] A.N. Gent and C.T.R. Pulford, *Journal of Materials Science* 1984; **19**:3612-3619.

[16] K. Tsunoda, J.J.C. Busfield, C.K.L. Davies and A.G. Thomas, *Journal of Materials Science* 2000; **35**:5187–5198.

[17] V. Le Saux, Y. Marco, S. Calloch, C. Doudard and P. Charrier. An energetic criterion for the fatigue of rubbers: an approach based on a heat build-up protocol and µ-tomography measurements. *Fatigue 2010 (Prague)*.

[18] V. Le Saux, Y. Marco, S. Calloch, C. Doudard and P. Charrier. Fast evaluation of the fatigue lifetime of elastomers based on a heat build-up protocol and micro-tomography measurements, *International Journal of Fatigue*, 2010, accepted.